J. Cent. South Univ. (2015) 22: 3189−3201
DOI: 10.1007/s11771-015-2856-4

Springer

Peristaltic transport of MHD Williamson fluid in an inclined asymmetric channel through porous medium with heat transfer

K. Ramesh, M. Devakar

Department of Mathematics, Visvesvaraya National Institute of Technology, Nagpur-440010, India

Abstract: The intention of this investigation is to study the effects of heat transfer and inclined magnetic field on the peristaltic flow of Williamson fluid in an asymmetric channel through porous medium. The governing two-dimensional equations are simplified under the assumption of long wavelength approximation. The simplified equations are solved for the stream function, temperature, and axial pressure gradient by using a regular perturbation method. The expression for pressure rise is computed numerically. The profiles of velocity, pressure gradient, temperature, heat transfer coefficient and stream function are sketched and interpreted for various embedded parameters and also the behavior of stream function for various wave forms is discussed through graphs. It is observed that the peristaltic velocity increases from porous medium to non-porous medium, the magnetic effects have increasing effect on the temperature, and the size of the trapped bolus decreases with the increasing of magnetic effects while the trend is reversed with the increasing of Darcy number. Moreover, limiting solutions of our problem are in close agreement with the corresponding results of the Newtonian fluid model.

Key words: Williamson fluid; heat transfer; inclined magnetic field; porous medium; inclined asymmetric channel

1 Introduction

Peristaltic flows are generated by the propagation of waves along the flexible walls of the channel/tube. These flows occur widely in many biological and biomedical systems, such as urine transport from kidneys to bladder, chyme movement in the gastrointestinal tract, transport of spermatozoa in the ductus efferent of the male reproductive tracts, movements of ovum in the female fallopian tube and circulation of blood in the small blood vessels. This mechanism also has many industrial applications like sanitary fluid transport and blood pumps in heart lung machine. Such flows are extensively studied in various geometries by using different assumptions of large wave length, small amplitude ratio, low Reynolds number, and etc. [1−6].

The interaction of peristalsis in the presence of magnetic field and heat transfer has attracted much attention to the researchers. Concept of heat transfer analysis is very useful in obtaining the blood flow rate through the initial thermal conditions and the thermal clearance rate. The flow of blood can be estimated by a dilation technique. In this procedure, heat is either injected or generated locally and the thermal clearance is monitored. Specifically, the bio heat transfer plays a key role in destroying undesirable tissues, hyperthermia, laser therapy and cryosurgery. Flow through porous medium has been of considerable interest in recent years because of its widespread applications in bio fluid mechanics. In view of this, many researchers have studied the peristaltic flows in different situations. ELMABOUD and MEKHEIMER [7], TRIPATHI and ANWAR [8], and EL SHEHAWAY and HUSSENY [9] have discussed the peristaltic problems through porous medium. NADEEM and AKRAM [10−11], WANG et al [12], SRINIVAS and PUSHPARAJ [13] and HAYAT et al [14−15] have investigated the problems on peristaltic flows under effect of magnetic field. NADEEM and AKBAR [16−17], NADEEM and AKRAM [18], MEHMOOD et al [19] and HAYAT et al [20] have studied the effect of heat transfer on the peristaltic transport under the magnetic field effects. SRINIVAS and MUTHURAJ [21] have analyzed the peristaltic flow situation through the porous medium under the effects of heat transfer and magnetic field.

The aim of the present work is to examine the influence of heat transfer and an inclined magnetic field on the Williamson fluid in an inclined asymmetric porous channel. The flow is generated by progressive waves with the channel walls.

2 Williamson fluid model

The governing equations for an incompressible fluid are given by

Received date: 2014−06−16; **Accepted date:** 2014−09−18
Corresponding author: M. Devakar, Professor; E-mail: m.devakar@yahoo.com

$$\mathrm{div}\bar{\boldsymbol{q}} = 0 \tag{1}$$

$$\rho\frac{\mathrm{d}\bar{\boldsymbol{q}}}{\mathrm{d}t} = \mathrm{div}\bar{\boldsymbol{\tau}} + \rho\bar{f} \tag{2}$$

where ρ is the density; $\bar{\boldsymbol{q}}$ is the velocity vector; $\bar{\boldsymbol{\tau}}$ is the Cauchy stress tensor; $\bar{f}$ represents the specific body force.

The constitutive equation for Williamson fluid is given by [6]

$$\bar{\boldsymbol{\tau}} = -\bar{P}_1 + \bar{\boldsymbol{S}} \tag{3}$$

$$\bar{\boldsymbol{S}} = [\mu_\infty + (\mu_0 + \mu_\infty)(1 - \Gamma\bar{\dot{\gamma}})^{-1}]\bar{\dot{\gamma}} \tag{4}$$

where $\bar{P}_1$ is the spherical part of the stress due to constraint of incompressibility; $\bar{\boldsymbol{S}}$ is the extra stress tensor; μ_∞ is the infinite shear rate viscosity; μ_0 is the zero shear rate viscosity; Γ is the time constant; $\bar{\dot{\gamma}}$ is defined as

$$\bar{\dot{\gamma}} = \sqrt{\frac{1}{2}\Sigma_i\Sigma_j\bar{\dot{\gamma}}_{ij}\bar{\dot{\gamma}}_{ji}} = \sqrt{\frac{1}{2}\boldsymbol{\Pi}} \tag{5}$$

where $\boldsymbol{\Pi}$ is the second invariant strain tensor. We consider the constitutive Eq. (4), the case for which $\mu_\infty = 0$ and $\Gamma\bar{\dot{\gamma}}$<1. Then, the component of extra stress tensor can be written as

$$\bar{\boldsymbol{S}} = \mu_0[(1 - \Gamma\bar{\dot{\gamma}})^{-1}]\bar{\dot{\gamma}} = \mu_0[(1 + \Gamma\bar{\dot{\gamma}})]\bar{\dot{\gamma}} \tag{6}$$

The Newtonian fluid model can be obtained by choosing Γ=0.

3 Mathematical formulation

In the present work, we consider the peristaltic transport of an incompressible Williamson fluid in a two-dimensional inclined asymmetric channel through the porous medium under the effect of heat transfer and inclined magnetic field. The peristaltic flow is generated by propagation of waves on the channel walls travelling with different amplitudes and phases but with the same constant speed c. We further assume that, the induced magnetic field is negligible under the assumption of low magnetic Reynolds number. In the Cartesian coordinate system $(\bar{X}, \bar{Y})$ the upper wall is H_1 and the lower wall is H_2. The heat transfer process is maintained by considering temperatures $\bar{T}_0$ and $\bar{T}_1$ to the lower and upper walls of the channel, respectively. The wall surfaces are chosen as

$$H_1(\bar{X}, t) = d_1 + a_1\cos\left[\frac{2\pi}{\lambda}(\bar{X} - ct)\right] \tag{7}$$

$$H_2(\bar{X}, t) = -d_2 + a_2\cos\left[\frac{2\pi}{\lambda}(\bar{X} - ct) + \phi\right] \tag{8}$$

where a_1 and a_2 are the waves amplitudes; λ is the wave length; d_1+d_2 is the channel width; c is the speed of propagation; t is the time; $\bar{X}$ is the direction of wave propagation. The phase difference ϕ varies in the range $0 \le \phi \le \pi$, in which $\phi = 0$ corresponds to symmetric channel with waves out of phase and $\phi = \pi$ corresponds to that with waves in phase, and further a_1, a_2, d_1, d_2 and ϕ satisfy the condition $a_1^2 + a_2^2 + 2a_1a_2\cos\phi \le (d_1 + d_2)^2$.

In laboratory frame, the governing equations for the two-dimensional motion of an incompressible Williamson fluid in an inclined channel through the porous medium with an inclined magnetic field are

$$\frac{\partial\bar{U}}{\partial\bar{X}} + \frac{\partial\bar{V}}{\partial\bar{Y}} = 0 \tag{9}$$

$$\rho\left(\frac{\partial}{\partial t} + \bar{U}\frac{\partial}{\partial\bar{X}} + \bar{V}\frac{\partial}{\partial\bar{Y}}\right)\bar{U} = -\frac{\partial\bar{P}}{\partial\bar{X}} + \frac{\partial\bar{S}_{\bar{X}\bar{X}}}{\partial\bar{X}} + \frac{\partial\bar{S}_{\bar{Y}\bar{Y}}}{\partial\bar{Y}} - \sigma B_0^2\cos\Theta(\bar{U}\cos\Theta - \bar{V}\sin\Theta) - \frac{\mu}{\kappa}\bar{U} + \rho g\sin\alpha \tag{10}$$

$$\rho\left(\frac{\partial}{\partial t} + \bar{U}\frac{\partial}{\partial\bar{X}} + \bar{V}\frac{\partial}{\partial\bar{Y}}\right)\bar{V} = -\frac{\partial\bar{P}}{\partial\bar{Y}} + \frac{\partial\bar{S}_{\bar{X}\bar{Y}}}{\partial\bar{X}} + \frac{\partial\bar{S}_{\bar{Y}\bar{Y}}}{\partial\bar{Y}} + \sigma B_0^2\sin\Theta(\bar{U}\cos\Theta - \bar{V}\sin\Theta) - \frac{\mu}{\kappa}\bar{V} + \rho g\cos\alpha \tag{11}$$

$$\rho\xi\left(\frac{\partial}{\partial t} + \bar{U}\frac{\partial}{\partial\bar{X}} + \bar{V}\frac{\partial}{\partial\bar{Y}}\right)\bar{T} = \kappa^*\left(\frac{\partial^2\bar{T}}{\partial\bar{X}^2} + \frac{\partial^2\bar{T}}{\partial\bar{Y}^2}\right) + \bar{U}_{\bar{X}}\bar{S}_{\bar{X}\bar{X}} + (\bar{U}_{\bar{Y}} + \bar{V}_{\bar{X}})\bar{S}_{\bar{X}\bar{Y}} + \bar{V}_{\bar{Y}}\bar{S}_{\bar{Y}\bar{Y}} \tag{12}$$

where ρ is the density; $\bar{U}$ and $\bar{V}$ are the velocity components; $\bar{P}$ is the pressure; σ is the electrical conductivity of the fluid; κ is the permeability parameter; B_0 is the magnetic field; Θ is the angle of inclination of magnetic field; α is the angle of inclination; $\bar{T}$ is the temperature; κ^* is the thermal conductivity.

Introducing a wave frame $(\bar{x}, \bar{y})$ moving with velocity c away from the fixed frame $(\bar{X}, \bar{Y})$ by the transformations

$$\bar{x} = \bar{X} - ct, \bar{y} = \bar{Y}, \bar{u} = \bar{U} - c, \bar{v} = \bar{V}, \bar{p}(\bar{x}, \bar{y}) = \bar{P}(\bar{X}, \bar{Y}, t) \tag{13}$$

where $\bar{U}$, $\bar{V}$ and $\bar{P}$ are the velocity components, pressure in the laboratory frame, respectively; $\bar{u}$, $\bar{v}$ and $\bar{p}$ are the velocity components, pressure in the wave frame, respectively.

After employing these transformations, Eqs. (9)−(12) can be reduced to

$$\frac{\partial\bar{u}}{\partial\bar{x}} + \frac{\partial\bar{v}}{\partial\bar{y}} = 0 \tag{14}$$

$$\rho\left(\bar{u}\frac{\partial}{\partial\bar{x}} + \bar{v}\frac{\partial}{\partial\bar{y}}\right)\bar{u} = -\frac{\partial\bar{p}}{\partial\bar{x}} + \frac{\partial\bar{s}_{\bar{x}\bar{x}}}{\partial\bar{x}} + \frac{\partial\bar{S}_{\bar{y}\bar{x}}}{\partial\bar{y}} -$$

$$\sigma B_0^2\cos\Theta((\overline{u}+c)\cos\Theta-\overline{v}\sin\Theta)-\frac{\mu}{\kappa}(\overline{u}+c)+\rho g\sin\alpha \tag{15}$$

$$\rho\left(\overline{u}\frac{\partial}{\partial\overline{x}}+\overline{v}\frac{\partial}{\partial\overline{y}}\right)\overline{v}=-\frac{\partial\overline{p}}{\partial\overline{y}}+\frac{\partial\overline{s}_{\overline{xy}}}{\partial\overline{x}}+\frac{\partial\overline{S}_{\overline{yy}}}{\partial\overline{y}}+\sigma B_0^2\sin\Theta((\overline{u}+c)\cos\Theta-\overline{v}\sin\Theta)-\frac{\mu}{\kappa}\overline{v}-\rho g\cos\alpha \tag{16}$$

$$\rho\xi\left(\overline{u}\frac{\partial}{\partial\overline{x}}+\overline{v}\frac{\partial}{\partial\overline{y}}\right)\overline{T}=\kappa^*\left(\frac{\partial^2\overline{T}}{\partial\overline{x}^2}+\frac{\partial^2\overline{T}}{\partial\overline{y}^2}\right)+\overline{u}_{\overline{x}}\overline{S}_{\overline{xx}}+(\overline{u}_{\overline{y}}+\overline{v}_{\overline{x}})\overline{S}_{\overline{xy}}+\overline{v}_{\overline{y}}\overline{S}_{\overline{yy}} \tag{17}$$

The non-dimensional quantities are:

$$x=\frac{\overline{x}}{\lambda},\quad y=\frac{\overline{y}}{d_1},\quad u=\frac{\overline{u}}{c},\quad v=\frac{\overline{v}}{c},\quad h_1=\frac{H_1}{a_1},\quad h_2=\frac{H_2}{d_1},$$

$$c=\frac{c\overline{\tau}}{\lambda},\quad S=\frac{d_1}{\mu c}\overline{S},\quad p=\frac{d_1^2}{\lambda\mu c}\overline{p},\quad \delta=\frac{d_1}{\lambda},\quad d=\frac{d_2}{d_1},$$

$$a=\frac{a_1}{a_2},\ Re=\frac{\rho c d_1}{\mu},\ Fr=\frac{c^2}{gd_1},\ We=\frac{\Gamma c}{d_1},\ Ha=\sqrt{\frac{\sigma}{\mu}}B_0 d_1,$$

$$Da=\frac{\kappa}{d_1^2},\quad Ec=\frac{c^2}{\xi(\overline{T}_1-\overline{T}_0)},\quad \psi=\frac{\overline{\psi}}{cd_1},\quad Pr=\frac{\mu\xi}{\kappa^*},\quad \theta=\frac{\overline{T}-\overline{T}_0}{\overline{T}_1-\overline{T}_0},\quad Br=EcPr.$$

Using the above dimensionless variables in Eqs. (14)−(17), we get

$$\delta\frac{\partial u}{\partial x}+\frac{\partial v}{\partial y}=0 \tag{18}$$

$$Re\delta\left(u\frac{\partial u}{\partial x}+\frac{1}{\delta}v\frac{\partial u}{\partial y}\right)=-\frac{\partial p}{\partial x}+\delta\frac{\partial S_{xx}}{\partial x}+\frac{\partial S_{yx}}{\partial y}-Ha^2\cos\Theta((u+1)\cos\Theta-v\sin\Theta)-\frac{1}{D_a}(u+1)+\frac{Re}{Fr}\sin\alpha \tag{19}$$

$$Re\delta^2\left(u\frac{\partial v}{\partial x}+\frac{1}{\delta}v\frac{\partial v}{\partial y}\right)=-\frac{\partial p}{\partial x}+\delta^2\frac{\partial S_{xy}}{\partial x}+\delta\frac{\partial S_{yy}}{\partial y}+\delta Ha^2\sin\Theta((u+1)\cos\Theta-v\sin\Theta)-\frac{\delta^2}{D_a}v+\delta\frac{Re}{Fr}\cos\alpha \tag{20}$$

$$RePr\delta\left(u\frac{\partial\theta}{\partial x}+\frac{1}{\delta}v\frac{\partial\theta}{\partial y}\right)=-\left(\delta^2\frac{\partial^2\theta}{\partial x^2}+\frac{\partial^2\theta}{\partial y^2}\right)+Br[\delta u_x S_{xx}+(u_y+\delta v_x)S_{xy}+v_y S_{yy}] \tag{21}$$

Introducing the non-dimensional stream function $\psi(x,y)$ such that $u=\frac{\partial\psi}{\partial y}$ and $v=-\delta\frac{\partial\psi}{\partial x}$ in the governing Eqs. (19)−(21), we get

$$Re\delta\left[\left(\frac{\partial\psi}{\partial y}\frac{\partial}{\partial x}-\frac{\partial\psi}{\partial x}\frac{\partial}{\partial y}\right)\frac{\partial\psi}{\partial y}\right]=-\frac{\partial p}{\partial x}+\delta\frac{\partial S_{xx}}{\partial x}+\frac{\partial S_{yx}}{\partial y}-Ha^2\cos\Theta\left[\left(\frac{\partial\psi}{\partial y}+1\right)\cos\Theta+\delta\frac{\partial\psi}{\partial x}\sin\Theta\right]-\frac{1}{Da}\left(\frac{\partial\psi}{\partial y}+1\right)+\frac{Re}{Fr}\sin\alpha \tag{22}$$

$$-Re\delta^3\left[\left(\frac{\partial\psi}{\partial y}\frac{\partial}{\partial x}-\frac{\partial\psi}{\partial x}\frac{\partial}{\partial y}\right)\frac{\partial\psi}{\partial x}\right]=-\frac{\partial p}{\partial y}+\delta^2\frac{\partial S_{xy}}{\partial x}+\delta\frac{\partial S_{yy}}{\partial y}+\delta Ha^2\sin\Theta\left[\left(\frac{\partial\psi}{\partial y}+1\right)\cos\Theta+\delta\frac{\partial\psi}{\partial x}\sin\Theta\right]+\frac{\delta^3}{Da}\frac{\partial\psi}{\partial x}-\delta\frac{Re}{Fr}\cos\alpha \tag{23}$$

$$ReFr\delta\left[\left(\frac{\partial\psi}{\partial y}\frac{\partial\theta}{\partial x}-\frac{\partial\psi}{\partial x}\frac{\partial\theta}{\partial y}\right)\right]=\left(\delta^2\frac{\partial^2\theta}{\partial x^2}+\frac{\partial^2\theta}{\partial y^2}\right)+Br[\delta\psi_{xy}S_{xx}+(\psi_{yy}-\delta^2\psi_{xx})S_{xy}-\delta\psi_{xy}S_{yy}] \tag{24}$$

with

$$S_{xx}=2[1+We\dot{\gamma}]\frac{\partial^2\psi}{\partial x\partial y} \tag{25}$$

$$S_{yx}=[1+We\dot{\gamma}]\left(\frac{\partial^2\psi}{\partial y^2}-\delta^2\frac{\partial^2\psi}{\partial x^2}\right) \tag{26}$$

$$S_{yy}=-2\delta[1+We\dot{\gamma}]\frac{\partial^2\psi}{\partial x\partial y} \tag{27}$$

where

$$\dot{\gamma}=\left[2\delta^2\left(\frac{\partial^2\psi}{\partial x\partial y}\right)^2+\left(\frac{\partial^2\psi}{\partial y^2}-\delta^2\frac{\partial^2\psi}{\partial x^2}\right)^2+2\delta^2\left(\frac{\partial^2\psi}{\partial x\partial y}\right)^2\right]^{1/2} \tag{28}$$

By using the long wave length (δ<<1) approximation, neglecting the coefficients of δ, Eqs. (22)−(24) become

$$\frac{\partial p}{\partial x}=\frac{\partial}{\partial y}\left[\frac{\partial^2\psi}{\partial y^2}+We\left(\frac{\partial^2\psi}{\partial y^2}\right)^2\right]-\left(Ha^2\cos^2\Theta+\frac{1}{Da}\right)\cdot\left(\frac{\partial\psi}{\partial y}+1\right)+\frac{Re}{Fr}\sin\alpha \tag{29}$$

$$\frac{\partial p}{\partial y}=0 \tag{30}$$

$$\frac{\partial^2\theta}{\partial y^2}=-Br\left[\left(\frac{\partial^2\psi}{\partial y^2}\right)^2+We\left(\frac{\partial^2\psi}{\partial y^2}\right)^3\right] \tag{31}$$

The corresponding dimensionless boundary conditions are defined as follows:

$$\psi=\frac{F}{2},\ \frac{\partial\psi}{\partial y}=-1,\ \theta=1 \text{ at } y=h_1 \tag{32}$$

$$\psi=-\frac{F}{2},\ \frac{\partial\psi}{\partial y}=-1,\ \theta=0 \text{ at } y=h_2 \tag{33}$$

4 Rate of volume flow

The volume flow rate in the fixed frame is given by

$$Q=\int_{H_2}^{H_1}\overline{U}(\overline{X},\overline{Y},t)\mathrm{d}\overline{Y} \tag{34}$$

where H_1 and H_2 are functions of $\overline{X}$ and t, respectively.

The above expression in wave frame becomes

$$q=\int_{h_2}^{h_1}\overline{u}(\overline{x},\overline{y})\mathrm{d}\overline{y} \tag{35}$$

where h_1 and h_2 are functions of $\overline{x}$ alone. From Eqs. (13), (34) and (35), we can write

$$Q=q+ch_1-ch_2 \tag{36}$$

The time-mean flow over time period T at fixed position $\overline{X}$ is defined as

$$\overline{Q}=\frac{1}{T}\int_0^T Q\mathrm{d}t \tag{37}$$

Using Eq. (36) into Eq. (37) and then integrating, we get

$$\overline{Q}=q+cd_1+cd_2 \tag{38}$$

If we define the dimensionless time-mean flows Φ and F,respectively, in the laboratory and wave frame as

$$\Phi=\frac{\overline{Q}}{cd_1},\ F=\frac{q}{cd_1} \tag{39}$$

From Eq. (38), we obtain

$$\Phi=F+1+d \tag{40}$$

and

$$F=\int_{h_2}^{h_1}\frac{\partial\psi}{\partial y}\mathrm{d}y=\psi[h_1(x))-\psi(h_2(x)] \tag{41}$$

where

$$h_1(x)=1+a\cos(2\pi x),\quad h_2(x)=-d-b\cos(2\pi x+\phi) \tag{42}$$

5 Perturbation solution

Equations (29)−(31) are coupled non-linear differential equations. The exact solution may be not possible and hence we focus our attention to finding the approximate analytical solution by regular perturbation method. For perturbation solution, we express ψ, θ and $\partial p/\partial x$ with the perturbation parameter We as

$$\psi=\psi_0+We\psi_1+O(We^2) \tag{43}$$

$$\theta=\theta_0+We\theta_1+O(We^2) \tag{44}$$

$$\frac{\partial p}{\partial x}=\frac{\partial p_0}{\partial x}+We\frac{\partial p_1}{\partial x}+O(We^2) \tag{45}$$

Invoking Eqs. (43)−(45) in Eqs. (29)−(31), and comparing the like power of We, we get the zeroth and first order systems and solving these equations we obtain the expressions of the stream function ψ, the temperature profile θ and the pressure gradient $\partial p/\partial x$ as

$$\begin{aligned}\psi=&B_1+B_2y+A_3\cosh(m_1y)+A_4\sinh(m_1y)+\\&We[C_5\cosh(m_1y)+C_6\sinh(m_1y)+C_7\cosh(2m_1y)+\\&C_8y^2+C_9y+C_{10}]\end{aligned} \tag{46}$$

$$\begin{aligned}\theta=&D_1\cosh(2m_1y)+D_2y^2+D_3y+D_4+\\&We[D_{19}\sinh(m_1y)\cosh(2m_1y)+D_{20}\sinh(2m_1y)\cdot\\&\cosh(m_1y)+D_{21}\sinh(2m_1y)\sinh(m_1y)+\\&D_{22}\cosh(2m_1y)\cosh(m_1y)+D_{23}\cosh(4m_1y)+\\&D_{24}\cosh(2m_1y)+D_{25}\cosh(m_1y)+\\&D_{26}\sinh(m_1y)+D_{27}y^2+D_{28}y+D_{29}]\end{aligned} \tag{47}$$

$$\begin{aligned}\frac{\partial p}{\partial x}=&-m_1^2(1+B_2)+\frac{Re}{Fr}\sin\alpha+We[6C_7m_1^3\sinh(2m_1y)+\\&B_3m_1^3\sinh(m_1y)+B_4m_1^3\cosh(m_1y)-(2C_8y+C_9)m_1^2]\end{aligned} \tag{48}$$

The coefficients of the heat transfer at the walls $y=h_1$ and $y=h_2$ respectively are given by [18]

$$Z_{h_1}=\frac{\partial h_1}{\partial x}\frac{\partial\theta}{\partial y},\ Z_{h_2}=\frac{\partial h_2}{\partial x}\frac{\partial\theta}{\partial y} \tag{49}$$

After using Eq. (47) in Eq. (49), we get the expressions for heat transfer coefficients as follows:

$$\begin{aligned}Z_{h_1}=&-2a\pi\sin(2\pi x)\{[2m_1D_1\sinh(2m_1y)+2D_2y+D_3]\cdot\\&We[m_1(2D_{19}+D_{20})\sinh(m_1y)\sinh(2m_1y)+\\&m_1(D_{19}+2D_{20})\cosh(m_1y)\cosh(2m_1y)+\\&m_1(2D_{21}+D_{22})\sinh(m_1y)\cosh(2m_1y)+\\&m_1(D_{21}+2D_{22})\sinh(2m_1y)\cosh(m_1y)+\\&4m_1D_{23}\sinh(4m_1y)+2m_1D_{24}\sinh(2m_1y)+\\&m_1D_{25}\sinh(m_1y)+m_1D_{26}\cosh(m_1y)+\\&2D_{27}y+D_{28}]\}\end{aligned} \tag{50}$$

$$\begin{aligned}Z_{h_2}=&2b\pi\sin(2\pi x+\phi)\{[2m_1D_1\sinh(2m_1y)+2D_2y+D_3]\cdot\\&We[m_1(2D_{19}+D_{20})\sinh(m_1y)\sinh(2m_1y)+\\&m_1(D_{19}+2D_{20})\cosh(m_1y)\cosh(2m_1y)+\\&m_1(2D_{21}+D_{22})\sinh(m_1y)\cosh(2m_1y)+\\&m_1(D_{21}+2D_{22})\sinh(2m_1y)\cosh(m_1y)+\\&4m_1D_{23}\sinh(4m_1y)+2m_1D_{24}\sinh(2m_1y)+\\&m_1D_{25}\sinh(m_1y)+m_1D_{26}\cosh(m_1y)+\\&2D_{27}y+D_{28}]\}\end{aligned} \tag{51}$$

The pressure rise Δ_{p_λ} per unit width of the channel in the non-dimensional form is given by

$$\Delta_{p_\lambda}=\int_0^1\left(\frac{\partial p}{\partial x}\right)_{y=0}\mathrm{d}x \tag{52}$$

6 Expressions for different wave shapes

The non-dimensional expressions for the four considered wave forms are given by the following equations.

1) Sinusoidal wave:

$$h_1(x)=1+a\sin(2\pi x) \tag{53}$$

$$h_2(x)=-d-b\sin(2\pi x+\phi) \tag{54}$$

2) Triangular wave:

$$h_1(x)=1+a\left\{\frac{8}{\pi^3}\sum_{n=1}^{\infty}\frac{(-1)^{n+1}}{(2n-1)^2}\sin[2\pi(2n-1)x]\right\} \tag{55}$$

$$h_2(x)=-d-b\left\{\frac{8}{\pi^3}\sum_{n=1}^{\infty}\frac{(-1)^{n+1}}{(2n-1)^2}\sin[2\pi(2n-1)x+\phi]\right\} \tag{56}$$

3) Square wave:

$$h_1(x)=1+a\left\{\frac{4}{\pi}\sum_{n=1}^{\infty}\frac{(-1)^{n+1}}{(2n-1)}\cos[2\pi(2n-1)x]\right\} \tag{57}$$

$$h_2(x)=-d-b\left\{\frac{4}{\pi}\sum_{n=1}^{\infty}\frac{(-1)^{n+1}}{(2n-1)}\cos[2\pi(2n-1)x+\phi]\right\} \tag{58}$$

4) Trapezoidal wave:

$$h_1(x)=1+a\left\{\frac{32}{\pi^2}\sum_{n=1}^{\infty}\frac{\sin\left(\frac{\pi}{8}(2n-1)\right)}{(2n-1)^2}\sin[2\pi(2n-1)x]\right\} \tag{59}$$

$$h_2(x)=-d-b\left\{\frac{32}{\pi^2}\sum_{n=1}^{\infty}\frac{\sin\left(\frac{\pi}{8}(2n-1)\right)}{(2n-1)^2}\sin[2\pi(2n-1)x+\phi]\right\} \tag{60}$$

7 Graphical results and discussion

This section describes the effect of various parameters on the velocity profile, temperature distribution, pressure gradient, heat transfer coefficient and stream lines through following figures. The limiting solutions of our investigation and pressure rise for different involved parameters are discussed through tables.

The variations of inclined magnetic field angle Θ, Darcy number *Da*, Hartmann number *Ha* and phase difference ϕ on the velocity have been plotted in Figs. 1(a)−(d). It is seen that the velocity increases near the center of the channel and decreases near the walls. Moreover, velocity increases in the middle of the channel from porous medium to non-porous. Figure 1(c) shows that an increasing *Ha* leads to decrease in velocity at the center of the channel and increase near the walls. That is, the presence of magnetic field decreases the fluid velocity in the middle part of the channel. The increase in ϕ decreases the velocity near the lower wall of the channel and the behavior is opposite near the other wall, which is shown in Fig. 1(d).

Figures 2(a)−(d) illustrate the variations of pressure gradient verses unit wavelength x with $x\in[0,1]$. From these figures, it can be seen that, by increasing inclined magnetic field angle Θ, phase difference ϕ, Darcy number *Da* and Hartmann number *Ha*, the relative pressure gradient is small in the wider part of the channel and large in the narrow part of the channel. It means that, in the wider part of the channel the fluid can easily move without imposition of larger pressure gradient but it has opposite behavior in the narrow part of the channel. Moreover, the pressure gradient decreases with increase in Θ, ϕ and *Da*, and the trend is reversed with *Ha*. The streamlines for various values of inclined magnetic field angle Θ, Darcy number *Da* and Hartmann number *Ha* are shown in the Figs. 3−5 for symmetric and asymmetric channels. From Figs. 3−4, it is clear that, as Θ and *Da* increase, the size of trapping bolus increases in the symmetric and asymmetric channels. For the same values of Θ and *Da*, with increasing ϕ, trapped bolus moves with the channel walls. It is depicted from Fig. 5 that, size of trapped bolus decreases with increase in *Ha*. Figures 6−7 represents that streamlines for various wave forms with phase difference ϕ. It is observed from the figures that, as ϕ increases from 0 to π, the size of trapped bolus decreases and moves to right with the wave; when ϕ reaches to π, the trapped bolus disappears.

Figure 8 is prepared to study the role of different parameters in the heat transfer coefficient on the upper wall. Figure 8(*a*) shows that the absolute value of heat transfer coefficient increases by increasing Hartmann number *Ha*. Figures 8(b)−(d) show that the heat transfer coefficient decreases in magnitude with an increasing of inclined magnetic angle Θ, Brinkman number *Br* and phase difference ϕ. Moreover, the heat transfer coefficient has oscillatory behavior.

Figure 9 represents the temperature profile for various parameters. From Figs. 9(a)−(b), it is evident that the temperature θ increases by increasing of Brinkman number *Br* and inclined magnetic angle Θ. The temperature decreases with an increasing in Hartmann

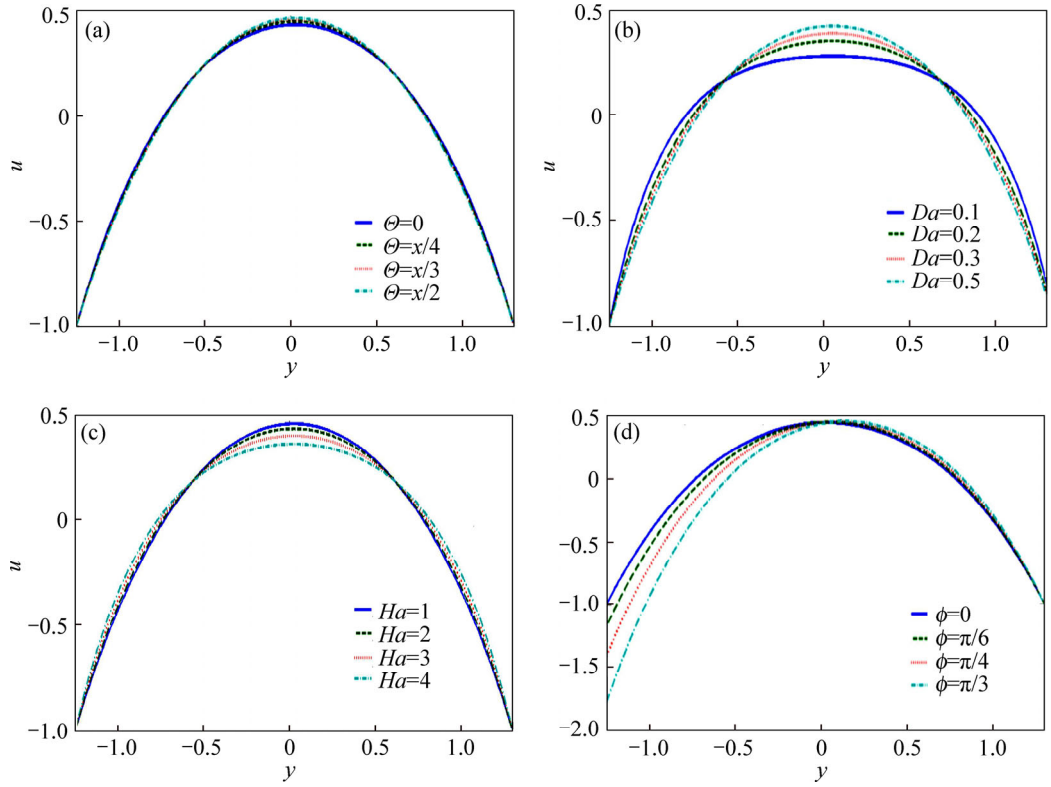

Fig. 1 Velocity profile for fixed values of (a) x=0, a=0.3, b=0.5, d=1, Φ=1, We=0.001, Ha=1, Da=1, ϕ=π/3; (b) x=0, a=0.3, b=0.5, d=1, Φ=1, We=0.001, Ha=1, Θ=π/3, ϕ=π/3; (c) x=0, a=0.3, b=0.5, d=1, Φ=1, We=0.001, Θ=π/3, Da=1, ϕ=π/3; (d) x=0, a=0.3, b=0.5, d=1, Φ=1, We=0.001, Ha=1, Da=1, Θ=π/3

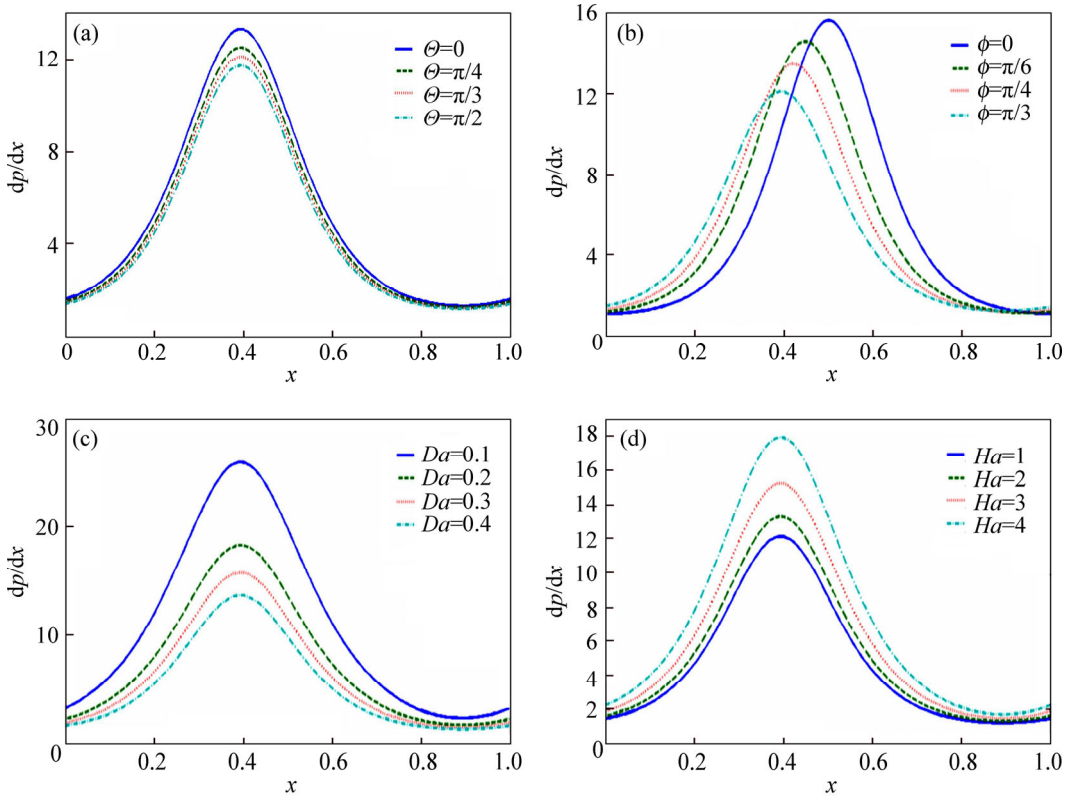

Fig. 2 Pressure gradient for fixed values: (a) y=0, a=0.3, b=0.5, d=1, Φ=1, We=0.001, Ha=1, Da=1, ϕ=π/3, Re=0.5, Fr=0.5, α=π/3; (b) y=0, a=0.3, b=0.5, d=1, Φ=1, We=0.001, Ha=1, Da=1, Θ=π/3, Re=0.5, Fr=0.5, α=π/3; (c) y=0, a=0.3, b=0.5, d=1, Φ=1, We=0.001, Ha=1, Θ=π/3, ϕ=π/3, Re=0.5, Fr=0.5, α=π/3; (d) y=0, a=0.3, b=0.5, d=1, Φ=1, We=0.001, Θ=π/3, Da=1, ϕ=π/3, Re=0.5, Fr=0.5, α=π/3

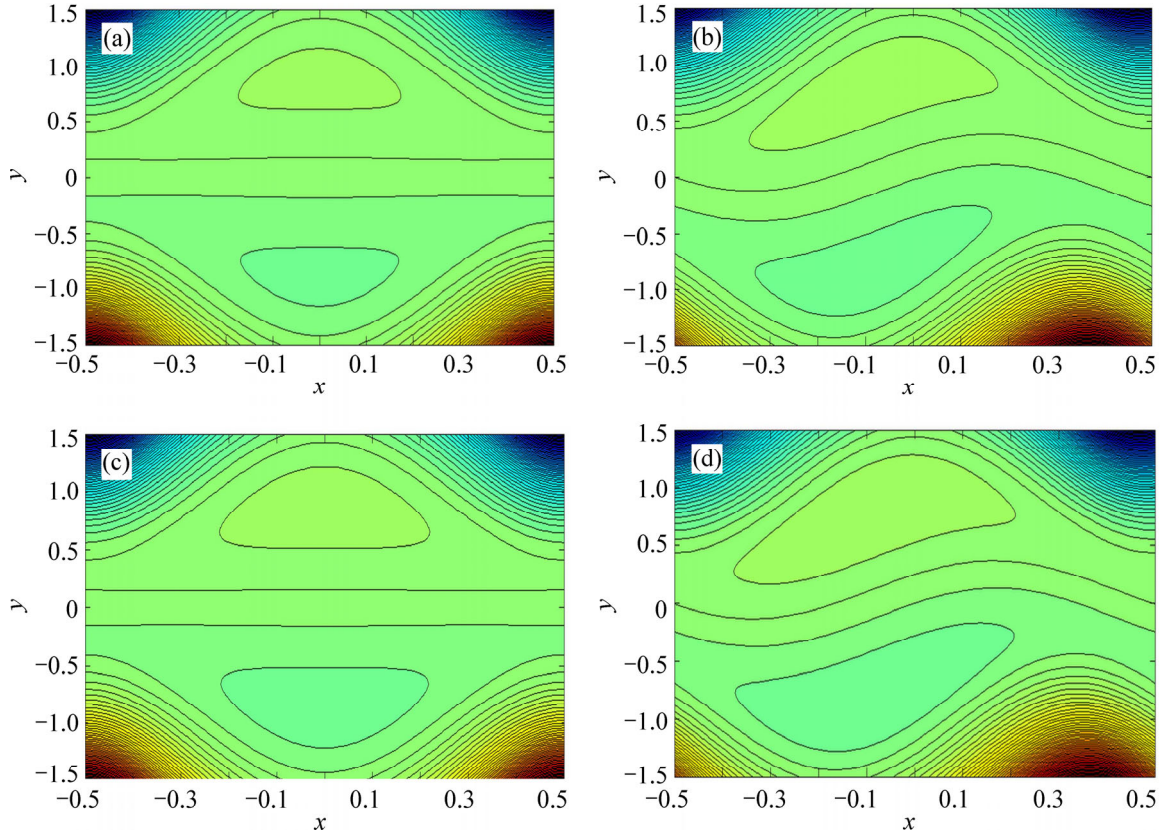

Fig. 3 Streamlines for fixed values of a=0.3, b=0.5, d=1, Φ=2, We=0.001, Ha=1, Da=1: (a) Θ=0, ϕ=0; (b) Θ=0, ϕ=π/3; (c) Θ=π/3, ϕ=0; (d) Θ=π/3, ϕ=π/3

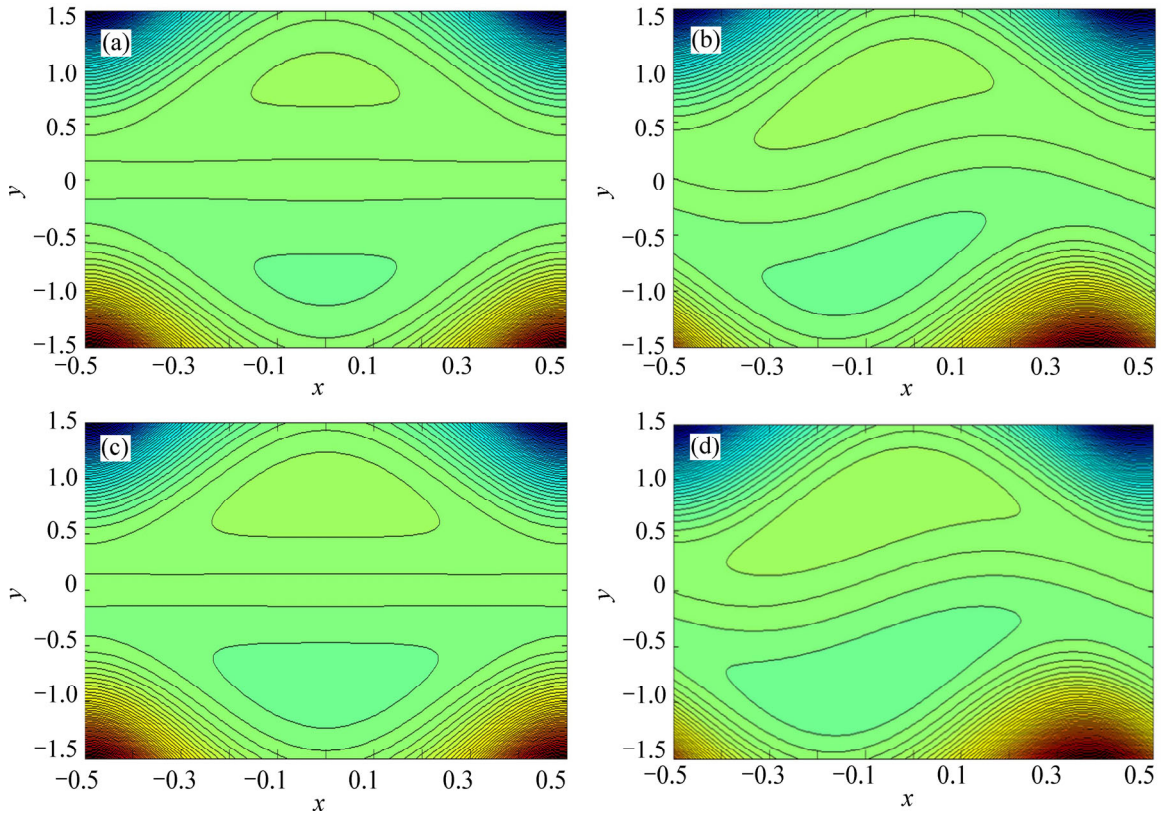

Fig. 4 Streamlines for fixed values of a=0.3, b=0.5, d=1, Φ=2, We=0.001, Ha=1, Θ=π/3: (a) Da=0.5, ϕ=0; (b) Da=0.5, ϕ=π/3; (c) Da=1.5, ϕ=0; (d) Da=1.5, ϕ=π/3

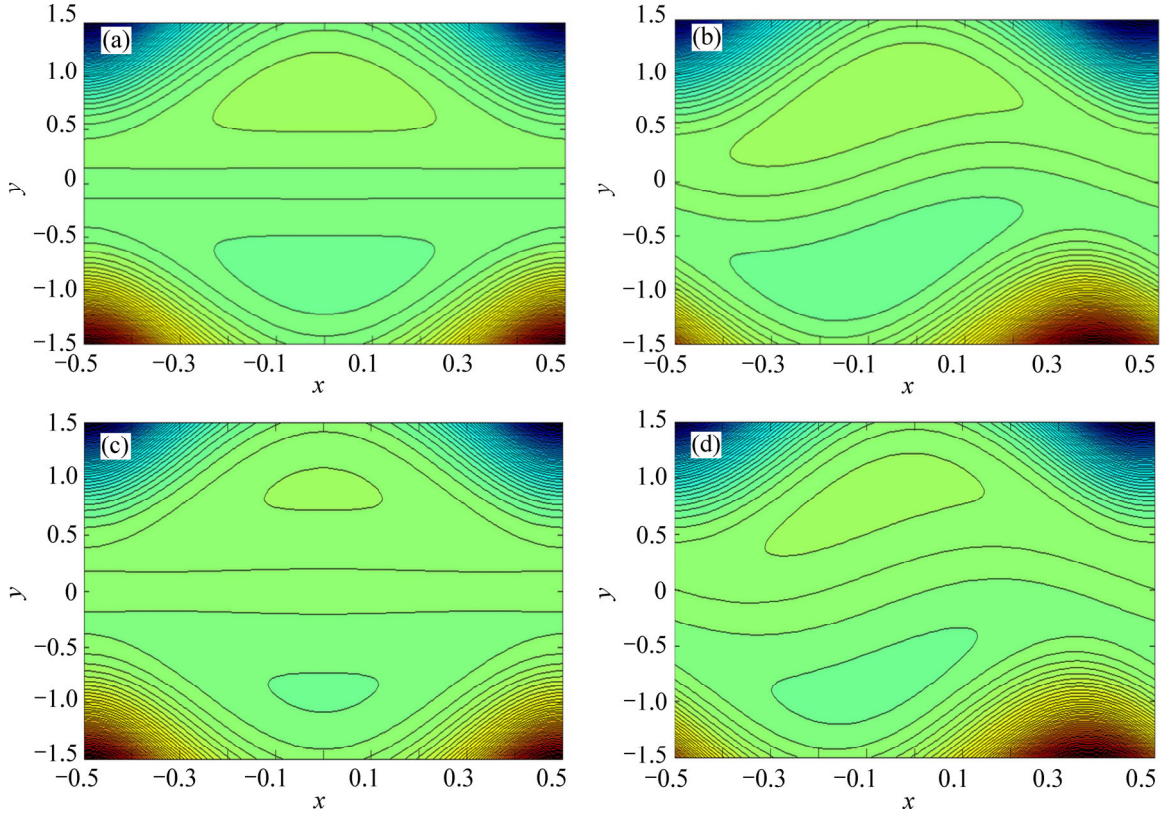

Fig. 5 Streamlines for fixed values of a=0.5, b=0.5, d=1, Φ=2, We=0.001, Da=1, Θ=π/3: (a) Ha=0, ϕ=0; (b) Ha=0, ϕ=π/3; (c) Ha=2.5, ϕ=0; (d) Ha=2.5, ϕ=π/3

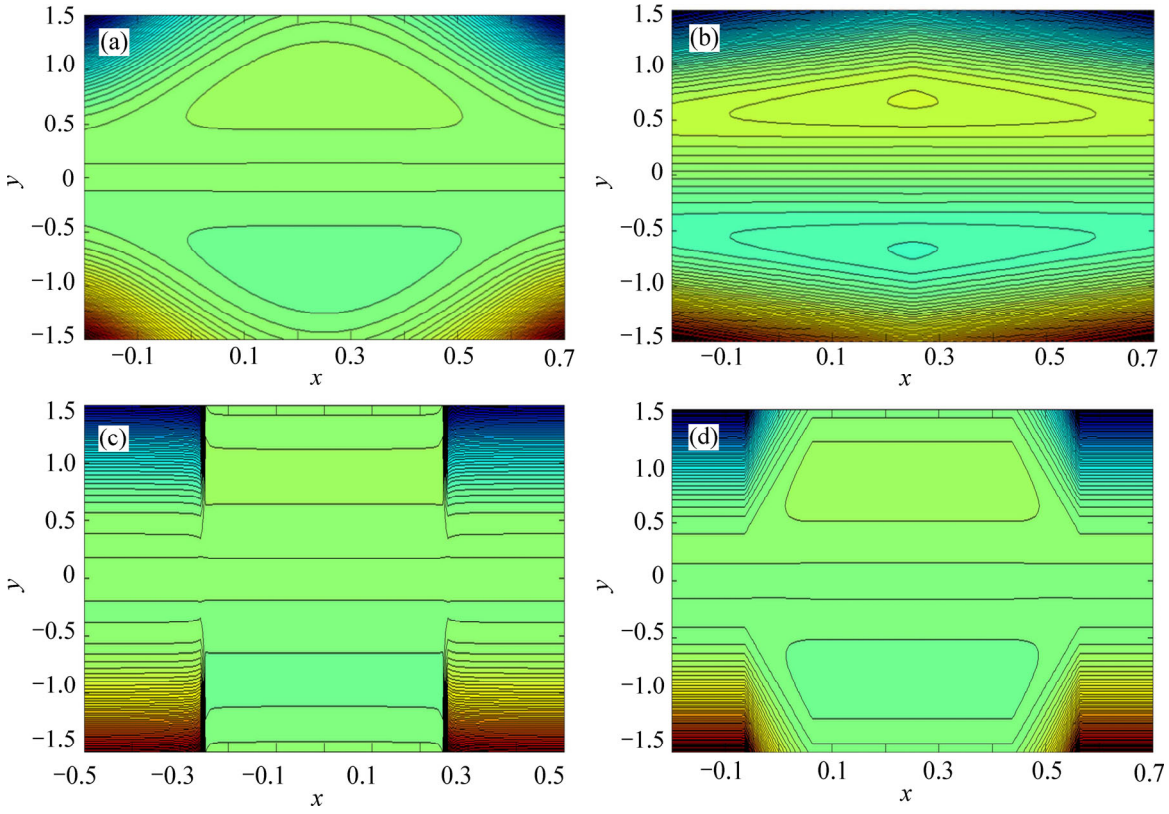

Fig. 6 Streamlines for various wave forms for fixed values of a=0.5, b=0.5, d=1, Φ=2, We=0.001, Ha=1, Da=1, Θ=π/3, ϕ=0: (a) Sinusoidal; (b) Triangular; (c) Square; (d) Trapezoidal

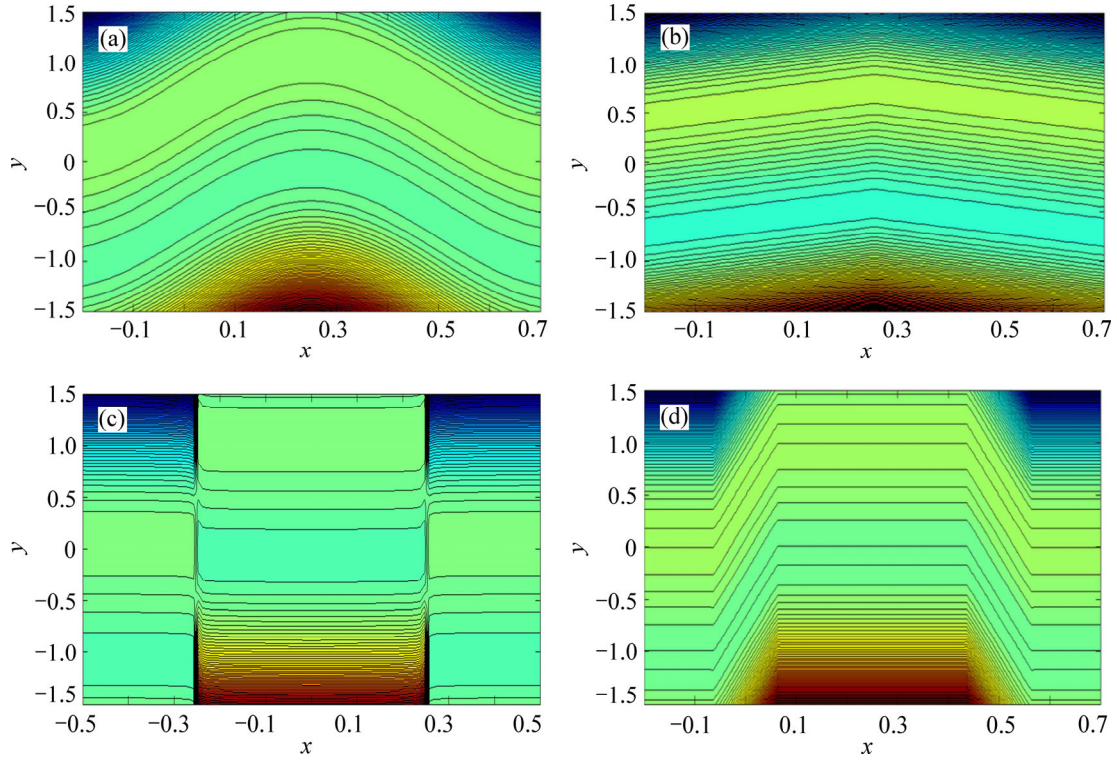

Fig. 7 Streamlines for various wave forms for fixed values of a=0.5, b=0.5, d=1, Φ=2, We=0.001, Ha=1, Da=1, Θ=π/3, ϕ=π: (a) Sinusoidal; (b) triangular; (c) Square; (d) Trapezoidal

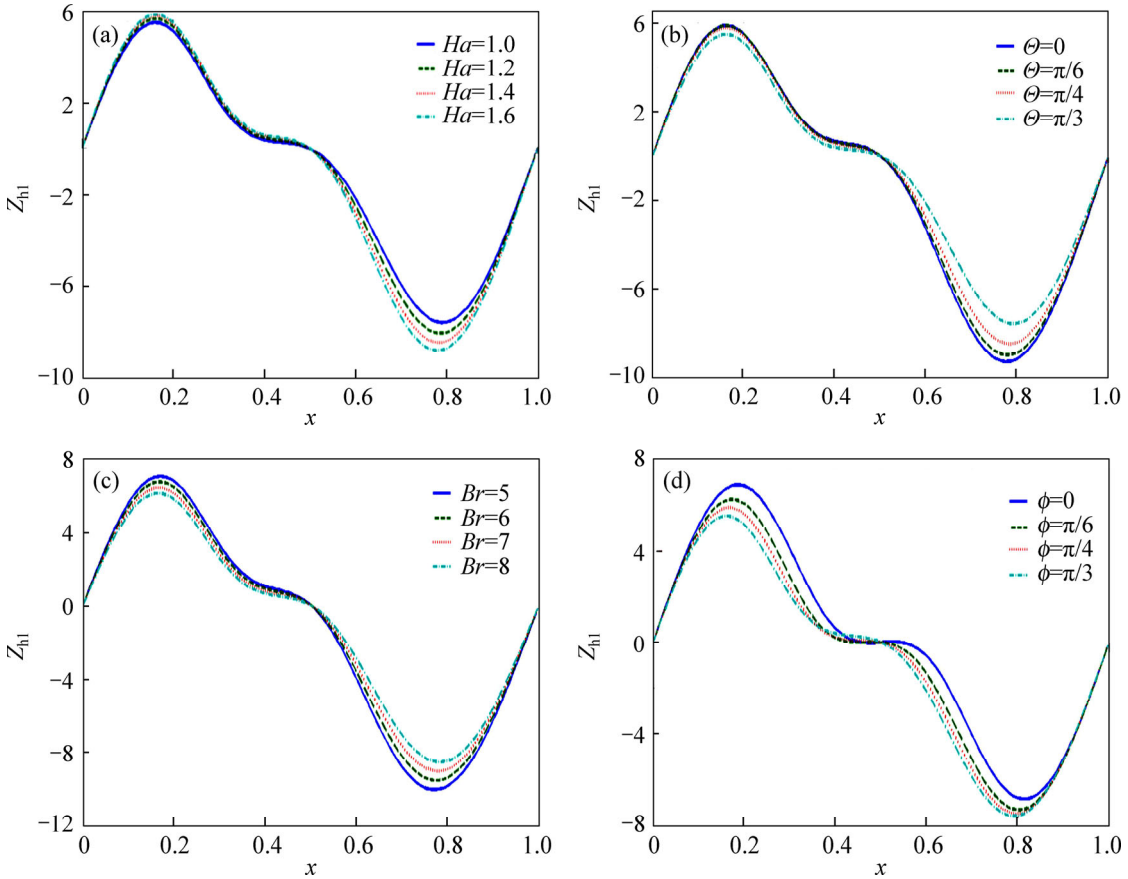

Fig. 8 Heat transfer coefficient at upper wall for fixed values: (a) a=0.3, b=0.5, d=1.5, Φ=1, We=0.001, Br=10, Da=1, Θ=π/3, ϕ=π/3; (b) a=0.3, b=0.5, d=1.5, Φ=1, We=0.001, Br=10, Da=1, Ha=1, ϕ=π/3; (c) a=0.3, b=0.5, d=1.5, Φ=1, We=0.001, Ha=1, Da=1, Θ=π/3, ϕ=π/3; (d) a=0.3, b=0.5, d=1.5, Φ=1, We=0.001, Br=10, Da=1, Θ=π/3, Ha=1

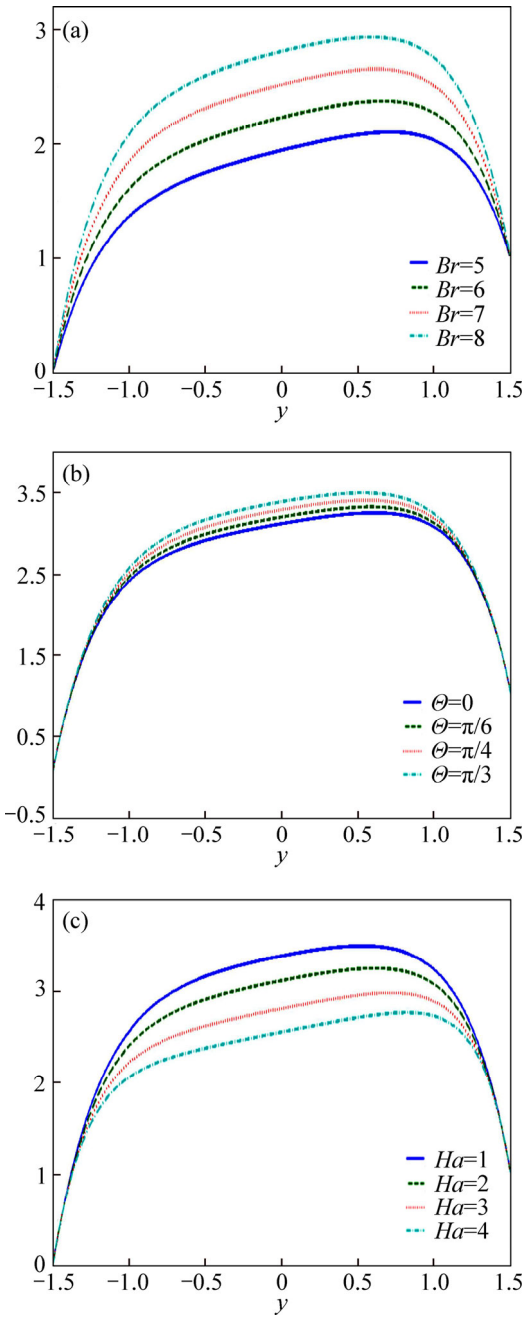

Fig. 9 Temperature profile for fixed values: (a) x=0, a=0.5, b=0.5, d=1, Φ=1, We=0.001, Ha=1, Da=1, ϕ=0, Θ=π/3; (b) x=0, a=0.5, b=0.5, d=1, Φ=1, We=0.001, Ha=1, Da=1, ϕ=0, Br=10; (c) x=0, a=0.5, b=0.5, d=1, Φ=1, We=0.001, Br=10, Da=1, ϕ=0, Θ=π/3

number Ha (see Fig. 9(c)). Moreover, in all the cases it is observed that the temperature profile is parabolic.

Table 1 gives the comparison of the present work with the earlier published work. In the absence of Weissenberg number, Darcy number and magnetic field, the present problem exactly matchs with the corresponding problem of Newtonian model [13]. Tables 2−5 represent the pressure rise for different values of Hartmann number, Darcy number, inclined angle of the channel and inclination magnetic field. It is observed from these tables that, as the Hartmann number increases, the pumping rate increases up to the critical value of Φ after

Table 1 Comparison of velocity profile when x=0, a=0.4, b=0.5, d=1, Φ=3, Ha=2, ϕ=π/3

y	$u(x, y)$ for present work when Θ=0, Da=0, We=0	$u(x, y)$ [13]
−1.25	−1.0000	−1.0000
−0.75	0.3643	0.3643
−0.25	0.8221	0.8221
0.25	0.8706	0.8706
0.75	0.5625	0.5625
1.25	−0.4367	−0.4367
1.40	−1.0000	−1.0000

Table 2 Variations of $\Delta_{p\lambda}$ verses Φ for a=0.4, b=0.5, d=1, Re=0.5, Fr=0.5, We=0.001, Θ=π/3, α=π/3, ϕ=π/3, Ec=0.5, Pr=5, Da=1

Φ	$\Delta_{p\lambda}$			
	Ha=1	Ha=2	Ha=3	Ha=4
−2	2.0657	2.2604	2.5838	3.0345
0	0.6225	0.6752	0.7626	0.8844
2	−0.8206	−0.9101	−1.0587	−1.2657

Table 3 Variations of $\Delta_{p\lambda}$ verses Φ for a=0.4, b=0.5, d=1, Re=0.5, Fr=0.5, We=0.001, Θ=π/3, α=π/3, ϕ=π/3, Ec=0.5, Pr=5, Da=1

Φ	$\Delta_{p\lambda}$			
	Da=0.1	Da=0.2	Da=0.3	Da=0.5
−2	4.3729	3.0986	2.6698	2.3252
0	1.2462	0.9017	0.7858	0.6927
2	−1.8807	−1.2952	−1.0982	−0.9398

Table 4 Variations of $\Delta_{p\lambda}$ verses Φ for a=0.4, b=0.5, d=1, Re=0.5, Fr=0.5, We=0.001, Ha=1, α=π/3, ϕ=π/3, Ec=0.5, Pr=5, Da=1

Φ	$\Delta_{p\lambda}$			
	Θ=0	Θ=π/4	Θ=π/3	Θ=π/2
−2	2.2604	2.1306	2.0657	2.0006
0	0.6752	0.6401	0.6225	0.6049
2	−0.9101	−0.8206	−0.8206	−0.7907

Table 5 Variations of $\Delta_{p\lambda}$ verses Φ for a=0.4, b=0.5, d=1, Re=0.5, Fr=0.5, We=0.001, Θ=π/3, Ha=1, ϕ=π/3, Ec=0.5, Pr=5, Da=1

Φ	$\Delta_{p\lambda}$			
	ϕ=0	ϕ=π/4	ϕ=π/3	ϕ=π/2
−2	1.9791	2.0497	2.0657	2.0791
0	0.5359	0.6066	0.6225	0.6359
2	−0.9072	−0.8365	−0.8205	−0.8072

that the situation is reversed. The effect of Darcy number and inclined magnetic field angle on pumping is opposite to that of Hartmann number. It can also be seen that the pumping rate is decreasing function of inclined angle of the channel. Moreover, as magnetic field increases, we get the best pumping results and there is better pumping rate in porous medium compared with non-porous medium. It is also noted that pumping performance is high in the vertical channel and low in the horizontal channel.

8 Conclusions

1) The fluid velocity increases from porous medium to non-porous medium.

2) The pressure gradient is an increasing function of Hartmann number and decreasing function of inclined angle of magnetic field, phase difference and Darcy number.

3) Increasing of inclination angle of the channel leads to increases in pumping rate.

4) The size of trapped bolus in triangular wave is smaller compared with other peristaltic waves.

5) The size of the trapped bolus decreases with the increasing of magnetic effects while it increases with the increasing of Darcy number.

6) The temperature increases with Hartmann number and the behavior is opposite in the inclined angle of magnetic field, phase difference and Darcy number.

7) Limiting case of our results is in close agreement with the corresponding results of Newtonian fluid model of former literature.

Acknowledgement

The authors are thankful to the anonymous reviewers for the encouraging comments.

Appendix:

$$m_1=\sqrt{Ha^2\cos^2\theta+\frac{1}{D_a}} \tag{61}$$

$$A_1=m_1^2[1+A_3m_1\sinh(m_1h_1)+A_4m_1\cosh(m_1h_1)] \tag{62}$$

$$A_2=m_1^2[-\frac{F}{2}-\frac{A_1h_1}{m^2}+A_4m_1\sinh(m_1h_1)+A_3m_1\cosh(m_1h_1)] \tag{63}$$

$$A_3=-\frac{A_4A_6}{A_5} \tag{64}$$

$$A_4=\frac{F+h_1-h_2}{A_7} \tag{65}$$

$$A_5=\sinh(m_1h_1)-\sinh(m_1h_2) \tag{66}$$

$$A_6=\cosh(m_1h_1)-\cosh(m_1h_2) \tag{67}$$

$$A_7=\left[m_1\cosh(m_1h_1)-\frac{A_6}{A_5}m_1\sinh(m_1h_1)\right](h_2-h_1)-\frac{A_6^2}{A_5}-A_5 \tag{68}$$

$$A_8=\sinh(2m_1h_1)-\sinh(2m_1h_2) \tag{69}$$

$$B_1=-\frac{A_2}{m^2} \tag{70}$$

$$B_2=-\frac{A_1}{m^2} \tag{71}$$

$$B_3=2m_1^6(A_3^2+A_4^2) \tag{72}$$

$$B_4=8A_3A_4m_1^6 \tag{73}$$

$$C_1=-m_1^2C_9 \tag{74}$$

$$C_2=-m_1^2(C_{10}-\frac{2C_4}{m_1^4}) \tag{75}$$

$$C_3=-\frac{1}{8m_1^2}(2B_3+B_4) \tag{76}$$

$$C_4=\frac{B_4}{4} \tag{77}$$

$$C_5=\frac{m_1A_6C_6+2m_1C_7C_8+2C_8(h_1-h_2)}{m_1A_5} \tag{78}$$

$$C_6=-\frac{C_{11}}{A_7} \tag{79}$$

$$C_7=\frac{c_3}{3m_1^2} \tag{80}$$

$$C_8=-\frac{c_4}{m_1^2} \tag{81}$$

$$C_9=\left[\frac{m_1A_6C_6+2m_1C_7C_8+2C_8(h_1-h_2)}{A_5}\right]\sinh(m_1h_1)-m_1C_6\cosh(m_1h_1)-2m_1C_7\sinh(2m_1h_1)-2C_8h_1 \tag{82}$$

$$C_{10}=-\frac{2C_4}{m_1^4}-\frac{C_2}{m_1^2} \tag{83}$$

$$C_{11}=\left[\frac{2m_1A_8C_7+2C_8(h_1-h_2)}{A_5}\sinh(m_1h_1)-2m_1C_7\sinh(2m_1h_1)-2C_8h_1\right](h_1-h_2)+C_7A_9+C_8(h_1^2-h_2^2)^2-\frac{2m_1A_6A_8C_7+2A_6C_8(h_1-h_2)}{m_1A_5} \tag{84}$$

$$D_1=-\frac{Brm_1^2}{8}(B_3^2+B_4^2+2B_3B_4) \tag{85}$$

$$D_2=-\frac{Brm_1^4}{4}(B_3^2-B_4^2-2B_3B_4) \tag{86}$$

$$D_3=\frac{1-D_1A_6-D_2(h_1^2-h_2^2)}{(h_1-h_2)} \tag{87}$$

$$D_4=1-D_1\cosh(2m_1h_1)-D_2h_1^2-D_3h_1 \tag{88}$$

$$D_5=-BrB_3^2m_1^6 \tag{89}$$

$$D_6=-BrB_4^2m_1^6 \tag{90}$$

$$D_7=-3BrB_3^2B_4m_1^6 \tag{91}$$

$$D_8=3BrB_4^2B_3m_1^6 \tag{92}$$

$$D_9=BrC_5^2m_1^4 \tag{93}$$

$$D_{10}=BrC_6^2m_1^4 \tag{94}$$

$$D_{11}=16BrC_7^2m_1^4 \tag{95}$$

$$D_{12}=2BrC_5C_6m_1^4 \tag{96}$$

$$D_{13}=8BrC_5C_7m_1^4 \tag{97}$$

$$D_{14}=8BrC_6C_7m_1^4 \tag{98}$$

$$D_{15}=4BrC_5C_8m_1^2 \tag{99}$$

$$D_{16}=4BrC_6C_8m_1^2 \tag{100}$$

$$D_{17}=16BrC_7C_8m_1^2 \tag{101}$$

$$D_{18}=4BrC_8^2 \tag{102}$$

$$D_{19}=\frac{1}{18m_1^2}(2D_5-D_6+6D_{14}) \tag{103}$$

$$D_{20}=\frac{1}{18m_1^2}(2D_6-D_5+8D_{14}) \tag{104}$$

$$D_{21}=\frac{1}{9m_1^2}(3D_7-2D_8-4D_{13}) \tag{105}$$

$$D_{22}=\frac{1}{18m_1^2}(5D_8-6D_7+10D_{13}) \tag{106}$$

$$D_{23}=\frac{D_{11}}{32m_1^2} \tag{107}$$

$$D_{24}=\frac{1}{8m_1^2}(D_9+D_{10}+D_{12}+2D_{17}) \tag{108}$$

$$D_{25}=\frac{1}{6m_1^2}(4D_5-3D_8+6D_{15}+D_5) \tag{109}$$

$$D_{26}=\frac{1}{6m_1^2}(3D_7-4D_6+6D_{16}-D_6) \tag{110}$$

$$D_{27}=\frac{1}{4}(D_9-D_{10}+D_{11}-D_{12}+2D_{18}) \tag{111}$$

$$\begin{aligned}D_{28}=\frac{1}{(h_2-h_1)}\{&D_{19}[\sinh(m_1h_1)\cosh(2m_1h_1)-\\&\sinh(m_1h_2)\cosh(2m_1h_2)]+D_{20}[\sinh(2m_1h_1)\cdot\\&\cosh(m_1h_1)-\sinh(2m_1h_2)\cosh(m_1h_2)]+\\&D_{21}[\sinh(m_1h_1)\sinh(2m_1h_1)-\sinh(m_1h_2)\cdot\\&\sinh(2m_1h_2)]+D_{22}[\cosh(m_1h_1)\cosh(2m_1h_1)-\\&\cosh(m_1h_2)\cosh(2m_1h_2)]+D_{23}[\cosh(4m_1h_1)-\\&\cosh(4m_1h_2)]+D_{24}[\cosh(2m_1h_1)-\\&\cosh(2m_1h_2)]+D_{25}[\cosh(m_1h_1)-\\&\cosh(m_1h_2)+D_{26}[\sinh(m_1h_1)-\\&\sinh(m_1h_2)]+D_{27}(h_1^2-h_2^2)\}\end{aligned} \tag{112}$$

$$\begin{aligned}D_{29}=-\{&D_{19}[\sinh(m_1h_1)\cosh(2m_1h_1)+\\&D_{20}\sinh(2m_1h_1)\cosh(m_1h_1)]+\\&D_{21}\sinh(m_1h_1)\sinh(2m_1h_1)+\\&D_{22}\cosh(m_1h_1)\cosh(2m_1h_1)+\\&D_{23}\cosh(4m_1h_1)+D_{24}\cosh(2m_1h_1)+\\&D_{25}\cosh(m_1h_1)+D_{26}\sinh(m_1h_1)+\\&D_{27}h_1^2+D_{28}h_1\}\end{aligned} \tag{113}$$

References

[1] MISHRA M, RAO A R. Peristaltic transport of a Newtonian fluid in an asymmetric channel [J]. Z Angew Math Phys, 2003, 54: 532−550.

[2] NASIR A L I, HAYAT T. Peristaltic flow of a micropolar fluid in an asymmetric channel [J]. Computers and Mathematics with Applications, 2008, 55: 589−608.

[3] NOREEN S, ALSAEDI A, HAYAT T. Peristaltic flow of pseudoplastic fluid in an asymmetric channel [J]. Journal of Applied Mechanics, 2012, 79: 1−6.

[4] NAGA R P, SAROJAMMA G. Peristaltic transport of a Casson fluid in an asymmetric channel [J]. Australasian Physical and Engineering Sciences in Medicine, 2004, 27: 49−59.

[5] HAYAT T, AMBREEN A, KHAN M, ASGHAR S. Peristaltic transport of a third order fluid under the effect of a magnetic field [J]. Computers and Mathematics with Applications, 2007, 53: 1074−1087.

[6] VAJRAVELU K, SREENADH S, RAJANIKANTH K, LEE C H. Peristaltic transport of a Williamson fluid in asymmetric channels with permeable walls [J]. Nonlinear Analysis: Real World Applications, 2012, 13: 2804−2822.

[7] ELMABOUD A Y, MEKHEIMER K H S. Non-linear peristaltic transport of a second order fluid through a porous medium [J]. Applied Mathematical Modelling, 2011, 35: 2695−2710.

[8] TRIPATHI D, ANWAR B O. A numerical study of oscillating peristaltic flow of generalized maxwell viscoelastic fluids through a porous medium [J]. Transp Porous Med, 2012, 95: 337−348.

[9] EL SHEHAWEY E F, HUSSENY S Z A. Effects of porous boundaries on peristaltic transport through a porous medium [J]. Acta Mechanica, 2000, 143: 165−177.

[10] NADEEM S, AKRAM S. Influence of inclined magnetic field on peristaltic flow of a Williamson fluid model in an inclined symmetric or asymmetric channel [J]. Mathematical and Computer Modelling, 2010, 52: 107−119.

[11] NADEEM S, AKRAM S. Peristaltic flow of a couple stress fluid under the effect of induced magnetic field in an asymmetric channel [J]. Arch Appl Mech, 2011, 81: 97−109.

[12] WANG Yong-qi, ALI N, HAYAT T. Peristaltic motion of a magnetohydrodynamic generalized second-order fluid in an

asymmetric channel [J]. Numerical Methods for Partial Differential Equations, 2009, 27: 415−435.

[13] SRINIVAS S, PUSHPARAJ V. Non-linear peristaltic transport in an inclined asymmetric channel [J]. Commun Nonlinear Sci Numer Simulat, 2008, 13: 1782−1795.

[14] HAYAT T, MAHOMED F M, ASGHAR S. Peristaltic flow of a magnetohydrodynamic Johnson-Segalman fluid [J]. Nonlinear Dynamics, 2005, 40: 375−385.

[15] HAYAT T, AFSAR A, KHAN M, ASGHAR S. Peristaltic transport of a third order fluid under the effect of a magnetic field [J]. Computers and Mathematics with Applications, 2007, 53: 1074−1087.

[16] NADEEM S, AKBAR N S. Influence of heat transfer on peristaltic transport of a Johnson-Segalman fluid in an inclined asymmetric channel [J]. Commun Nonlinear Sci Numer Simulat, 2010, 15: 2860−2877.

[17] NADEEM S, AKBAR N S. Effects of induced magnetic field on peristaltic flow of Johnson-Segalman fluid in a vertical symmetric channel [J]. Appl Math Mech Engl Ed, 2010, 31(8): 969−978.

[18] NADEEM S, AKRAM S. Magnetohydrodynamic peristaltic flow of a hyperbolic tangent fluid in a vertical asymmetric channel with heat transfer [J]. Acta Mech Sin, 2011, 27(2): 237−250.

[19] MEHMOOD O U, MUSTAPHA N, SHAFIE S. Heat transfer on peristaltic flow of fourth grade fluid in inclined asymmetric channel with partial slip [J]. Appl Math Mech Engl Ed, 2012, 33(10): 1313−1328.

[20] HAYAT T, SALEEM N, ASGHAR S, ALHOTHUALI M S, ALHOMAIDAN A. Influence of induced magnetic field and heat transfer on peristaltic transport of a Carreau fluid [J]. Commun Nonlinear Sci Numer Simulat, 2011, 16: 3559−3577.

[21] SRINIVAS S, MUTHURAJ R. Effects of chemical reaction and space porosity on MHD mixed convective flow in a vertical asymmetric channel with peristalsis [J]. Mathematical and Computer Modelling, 2011, 54: 1213−1227.

(Edited by DENG Lü-xiang)